CHIN.PHYS.LETT. Vol. 25, No. 9 (2008) 3300

Laser Induced Damage Threshold at 355 and 1064 nm of Ta_2O_5 Films of Different Phases

XU Cheng(许程)[1,2**], LI Xiao(李笑)[1,2], DONG Hong-Cheng(董洪成)[1,2], JIN Yun-Xia(晋云霞)[1], HE Hong-Bo(贺洪波)[1], SHAO Jian-Da(邵建达)[1], FAN Zheng-Xiu(范正修)[1]

[1]*Shanghai Institute of Optics and Fine Mechanics, Chinese Academy of Sciences, Shanghai 201800*
[2]*Graduate School of Chinese Academy of Sciences, Beijing 100049*

(Received 30 March 2008)

Ta_2O_5 films are deposited on fused silica substrates by conventional electron beam evaporation method. By annealing at different temperatures, Ta_2O_5 films of amorphous, hexagonal and orthorhombic phases are obtained and confirmed by x-ray diffractometer (XRD) results. X-ray photoelectron spectroscopy (XPS) analysis shows that chemical composition of all the films is stoichiometry. It is found that the amorphous Ta_2O_5 film achieves the highest laser induced damage threshold (LIDT) either at 355 or 1064 nm, followed by hexagonal phase and finally orthorhombic phase. The damage morphologies at 355 and 1064 nm are different as the former shows a uniform fused area while the latter is centred on one or more defect points, which is induced by different damage mechanisms. The decrease of the LIDT at 1064 nm is attributed to the increasing structural defect, while at 355 nm is due to the combination effect of the increasing structural defect and decreasing band gap energy.

PACS: 42.79.−e, 68.60.−p, 81.15.Ef

The laser induced damage threshold (LIDT) of optical films has become more important upon the increasing of the high average output and high peak power of lasers. Unfortunately, the mechanism of damage initiation has not been fully understood as it is complicated and associated with many factors.[1] For the nanosecond pulse laser, the damage of films has always been induced by defects, and the LIDT can be improved by decreasing the density or enhancing the mechanical stability of defects.[2,3] The detailed damage mechanism is different and should be discussed according to different cases. Previous reports show that much attention has been extensively paid on the effect of deposition methods and conditions, post-treatment, laser characteristics, coating designs and substrates on the LIDT of films.[4−7] To our best knowledge, little has been studied about the LIDT of films of different phases. Moreover, it is helpful for better known of the damage mechanism to investigate the LIDT at different wavelengths.[8,9]

Ta_2O_5 is one of the most extensively studied transition-metal oxides. It is a well-known optical material with high index and good quality that shows low loss, high stability, and a broad spectral range of high transparency. These outstanding properties make it widely benefit many scientific and technological branches, especially optical films for laser. However, the significant limitations for Ta_2O_5 films are the chemical substoichiometry and low LIDT, which always reduces their application in high-power laser systems.[10] In this study, Ta_2O_5 films are deposited on fused silica with conventional electron beam evaporation method and then annealed in air at different temperatures to obtain different phases of films. The chemical composition, transmittance, band gap energy, especially the LIDT at 355 and 1064 nm of Ta_2O_5 films of different phases are investigated.

The films were deposited by using Ta_2O_5 crushed aggregates as starting material with the purity of 99.99%. Ta_2O_5 films with an optical thickness of 6 QWOT (quarter wavelength optical thickness) at wavelength 550 nm were prepared on fused silica substrates under optical control. Before deposition, the chamber was pumped to a base pressure of 2×10^{-3} Pa and oxygen was introduced to keep oxygen partial pressure of 2×10^{-2} Pa. The substrate temperature was held at 573 K and the deposition rate was 0.32 nm/s. Annealing of films was performed in air at 873, 1073 and 1273 K for 8 h, respectively. Structure of Ta_2O_5 films was analysed by x-ray diffractometer (XRD). The composition of films were analysed by x-ray photoelectron spectroscopy (XPS) using focused monochromatic Al $K\alpha$ ($h\nu = 1486.6$ eV) radiation at a pass energy of 20 eV. Transmittance spectra of films were measured using a Lambda 900 spectrophotometer and the measurement error was within 0.08%. Thickness of films was measured by surface profilograph. Damage testing was performed in the one-on-one regime according to ISO standard 11254-1, using a Q-switched Nd:YAG pulsed laser.[11] The pulse length of the 355 and 1064 nm laser was 8 and 12 ns, respectively.[12,13] Ten sites of the sample were exposed at the same fluence and the fraction of the sites which were damaged was recorded. This procedure was repeated for other fluence until the range of fluence was sufficiently broad to include points of zero

**Email: xucheng@siom.ac.cn
© 2008 Chinese Physical Society and IOP Publishing Ltd

damage probability and points of 100% damage probability to develop a plot of damage probability versus fluence. The LIDT was defined as the incident pulse's energy density when the damage occurred at 0% damage possibility (J/cm^2), and it could be obtained by linear extrapolation of the damage possibility data to zero damage possibility.

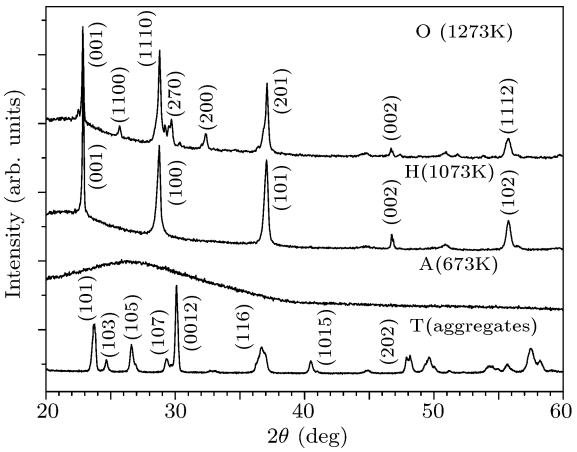


Fig. 1. XRD patterns of Ta_2O_5 aggregates and films (T-tetragonal, A-amorphous, H-hexagonal, O-orthorhombic).

Figure 1 shows XRD patterns of Ta_2O_5crushed aggregates and films annealed at different temperatures. The aggregate is tetragonal α-Ta_2O_5 according to the Joint Committee for Powder Diffraction Studies (JCPDS) data (Card 21-1119). During evaporation process, amorphous films are obtained and the film annealed at 873 K is still amorphous as shown in Fig. 1. When annealed at 1073 K, XRD analysis reveals the preferred formation of hexagonal δ-Ta_2O_5 phase (Card 19-1299).[14] The film becomes strongly crystallized showing the most intense (001), (100) and (101) reflections at $2\theta = 23.2$, 28.5 and 36.9°, respectively. In addition, the (002) and (110) reflections with lower intensity appear at 47.0 and 50.5°, respectively. The film annealed at 1273 K exhibits two distinct XRD reflection peaks at 28.4 and 28.7°, which is attributed to the (1110) and (200) reflection of orthorhombic β-Ta_2O_5 phase (Card 25-0922).[14,15] However, since all peaks originated from hexagonal phase spectrum can be assigned to orthorhombic phase as well, the orthorhombic phase cannot be identified on the basis of XRD alone. Considering that the temperature of orthorhombic phase transition is between 1073 and 1273 K reported by many previous researches and in this study the annealing is held at 1273 K for 8 h, we believe that little hexagonal phase exists except orthorhombic phase. The average grain sizes of films are calculated by Scherrer's equation:

$$D = \frac{0.89\lambda}{\beta \cos\theta}, \tag{1}$$

where D is the grain size, λ is the x-ray wavelength used by diffractometer, β is the full width at half-maximum of diffraction peak (FWHM), and θ is the Bragg diffraction angle. Thereinto, $\lambda = 0.15418$ nm. The grain sizes of Ta_2O_5 films of different phases are shown in Table 1. It is demonstrated that the grain sizes of hexagonal and orthorhombic Ta_2O_5films are 62 and 82 nm, respectively.

Table 1. Average grain sizes of Ta_2O_5 films of different phases.

Phases	2θ (deg)	β (deg)	D (nm)
Amorphous			
Hexagonal	22.8669	0.1301	62
Orthorhombic	22.8425	0.0973	82

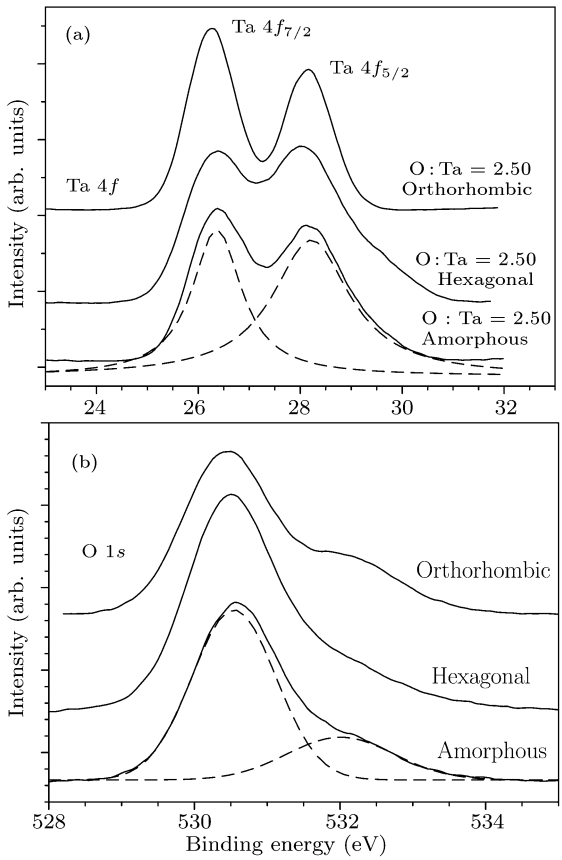


Fig. 2. High resolution XPS spectra of samples: (a) Ta 4f and (b) O1s.

All films are examined by high-resolution XPS in order to obtain the chemical composition. Figure 2(a) shows the Ta 4f spectra from samples. Curve fitting reveals two $4f_{7/2}$ and $4f_{5/2}$ peaks at 26.4 and 28.2 eV, respectively, which shows composition of films is Ta^{5+}.[16] Figure 2(b) shows that the two peaks fitted from O 1s spectra point to the presence of different chemical environments. The lower binding energy peak at 530.6 eV is due to Ta-O bonds, indicating the presence of Ta_2O_5. The peak at higher binding energy of 532.0 eV is usually attributed to surface contamination.[17] The O/Ta ratio is estimated from

the XPS peak areas together with their relative sensitivity factors. It is shown that all the O/Ta ratio of films is 2.50, which means that they are stoichiometry.

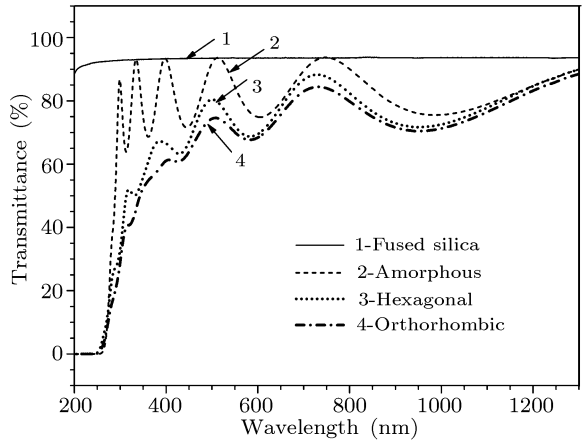


Fig. 3. Transmittance curves of samples.

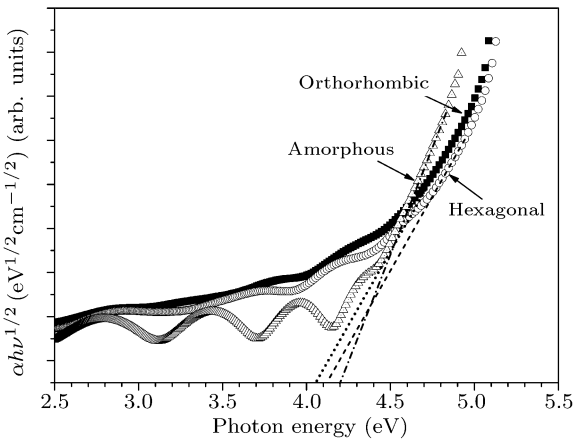


Fig. 4. $(\alpha h\nu)^{1/2}$ versus energy plots of samples.

Figure 3 represents the transmittance spectra of samples. The amorphous Ta_2O_5 film shows perfect transmittance, while the transmittance of crystalline Ta_2O_5 films decreases especially in the short wavelength region. It is mainly due to the crystal growth in films. The band gap energy E_g of films is calculated from Tauc formula:[18]

$$\alpha = B\frac{(h\nu - E_g)^2}{h\nu}, \tag{2}$$

where B is a constant related to the densities of states in the conduction and the valence band, α is absorption coefficient, and $h\nu$ is photon energy. E_g of Ta_2O_5films is obtained by plotting $(\alpha h\nu)^{1/2}$ versus $h\nu$ and extrapolating the linear portion of the spectrum for $\alpha = 0$. Absorption coefficient α is mainly influenced by two factors: (1) scattering losses and (2) intrinsic absorption. At shorter wavelength close to the band gap, the influence of intrinsic absorption on α is more prominent than scattering losses and α may be obtained by[19]

$$\alpha = \frac{1}{d}\ln\left(\frac{1}{T}\right), \tag{3}$$

where d is the thickness of films and T is the transmittance. Figure 4 illustrates plots of $(\alpha h\nu)^{1/2}$ against $h\nu$ in accordance with Eq. (2). The thickness d and E_g of films are given in Table 2. It shows that E_g of the amorphous film is 4.20 eV near the previous reports.[20−21] E_g of hexagonal and orthorhombic films decrease, are 4.12 and 4.05 eV, respectively.

Table 2. Thickness d and E_g of samples.

Phases	d (nm)	E_g (eV)
Amorphous	415	4.20
Hexagonal	410	4.12
Orthorhombic	403	4.05

Figure 5 illustrates the LIDT of samples. The amorphous film has the highest LIDT among the three samples either at the wavelength of 355 or 1064 nm. The LIDT of hexagonal film decreases, and the orthorhombic film achieves the lowest LIDT. In addition, the LIDT at 355 nm is lower than that at 1064 nm for all samples.

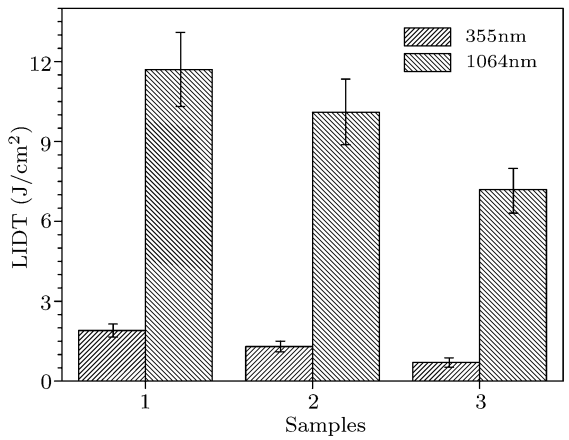


Fig. 5. LIDT results at 355 and 1064 nm of samples.

The film morphologies are observed with a Leica-DMRXE micropolariscope. Figures 6(a), 6(d) and 6(g) show that when the amorphous film transforms to crystalline film, the surface becomes more rough due to the crystal growth in the phase transition process. Although the surface roughness of the film increases significantly, the bulk structure of the film has not been broken, which can be attributed to the high temperature resistance of Ta_2O_5.[22] In addition, it can be found from Fig. 6 of some difference between the damage morphologies at 355 nm and 1064 nm. When damaged at 355 nm, it exhibits a uniform fused area without apparent defect points. However, at 1064 nm the damage areas are centred on one or more defect points.

The only model used to interpret damage statistics

in the nanosecond laser pulse regime until now is based on a physical assumption that a damage site is linked to the presence of at least one defect.[23] As the defect has a larger absorption index than the film around, it is more liable to absorb the laser energy. The temperature of the defect under the laser radiation increases to the melting or boiling point fast, thus the film would be damaged from the defect points. There are two kinds of defects in films, substoichiometric and structural defects, which would weaken the LIDT significantly.[24,25] As XPS results show that all the films are stoichiometry, the structural defect will be the dominant factor in LIDT. The decreased LIDT at the two wavelengths of Ta_2O_5 films can be explained as follows: when the film transforms from amorphous phase to crystalline phase, the crystal grain grows up accompanied with the increase of defect such as grain boundary. Thus, the LIDT of crystalline film decreases and is lower than that of amorphous film. In addition, the grain size of orthorhombic film (82 nm) is larger than that of hexagonal film (62 nm), resulting in the increased defect and lower LIDT.

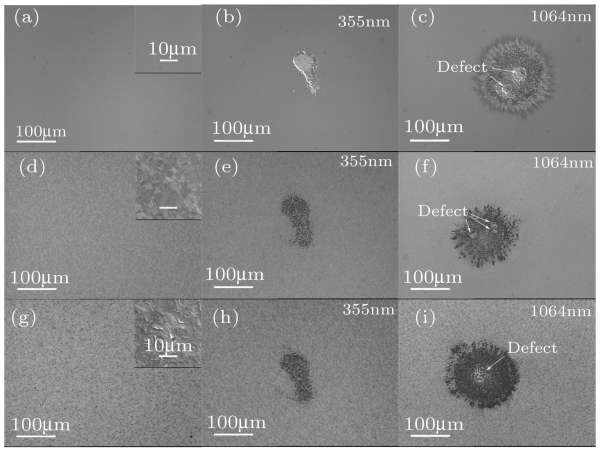


Fig. 6. Undamaged and damaged morphologies at 355 and 1064 nm of amorphous films (a)–(c), hexagonal films (d)–(f) and orthorhombic films (g)–(i).

Moreover, as the photon energy of 355 nm laser is 3.50 eV near E_g of Ta_2O_5, the intrinsic absorption of the film will also contribute to the initiation of damage. The reduced E_g will increase the intrinsic absorption and decrease the LIDT at 355 nm. Therefore, the mechanism is different between the damage of Ta_2O_5 films at 355 and 1064 nm. The initiation of damage at 1064 nm is merely dominated by defect, while at 355 nm it is dominated by the combination effect of defect and E_g of films. It is the reason why defect points in the damage morphology at 355 nm become less apparent than that at 1064 nm. Similar damage morphologies are also found for TiO_2 films damaged at 355 nm and most oxide films at 266 nm.[26] As E_g is the least and the defect density is the highest, the LIDT at 355 nm of orthorhombic film is the minimum. The lower LIDT of films at 355 nm compared to 1064 nm is due to the stronger absorption of defect at shorter wavelength.[27] Detailed damage mechanism at the two wavelengths is in our further research.

In summary, Ta_2O_5 films of amorphous, hexagonal and orthorhombic phases are obtained by annealing at different temperatures. The chemical composition, transmittance, band gap energy and LIDT of Ta_2O_5 films are investigated. Amorphous Ta_2O_5 films achieve the highest LIDT either at 355 or 1064 nm, followed by hexagonal phase and finally orthorhombic phase. Moreover, damage morphologies are different at different wavelengths, as it shows a uniform fused area at 355 nm whereas the damage is centred on one or more defect points at 1064 nm. The damage initiation at 1064 nm can be attributed to defect, while the damage at 355 nm is due to the combination effect of defect and E_g of films.

References

[1] Yuan L et al 2007 *J. Opt. Soc. Am.* B **24** 538
[2] Zhang D P et al 2004 *Opt. Lett.* **29** 2870
[3] Zhao Y A et al 2005 *Proc. SPIE* **5991** 599117-1
[4] Yu H et al 2007 *Appl. Surf. Sci.* **253** 6113
[5] Xu C, Yao J K, Ma J Y, Jin Y X and Shao J D 2007 *Chin. Opt. Lett.* **5** 727
[6] Xu C et al 2008 *Opt. Laser Technol.* **40** 545
[7] Xu C et al 2008 *Chin. Phys. Lett.* **25** 1321
[8] Natoli J Y et al 2005 *Opt. Lett.* **30** 1315
[9] Kouta H 1999 *Appl. Opt.* **38** 545
[10] Wolfe C R et al 1989 *Proc. SPIE* **509** 255
[11] ISO 11254-1:2000 Lasers and Laser-Related Equipment-Determination of Laser-Induced Damage Threshold of Optical Surfaces (Part 1.1-on-1 test)
[12] Zhan M Q et al 2006 *Opt. Eng.* **45** 063801
[13] Hu H, Fan Z and Luo F 2001 *Appl. Opt.* **40** 1950
[14] Dimitrova T et al 2001 *Thin Solid Films* **381** 31
[15] Gonzalez J et al 1998 *J. Mater. Sci.* **33** 4173
[16] Szymanowski H, Zabeida O, Klemberg-Sapieha J E and Martinu L 2005 *J. Vac. Sci. Technol.* A **23** 241
[17] Atanassova E et al 2002 *Microelectron. J.* **33** 907
[18] Tauc J 1974 *Amorphous and Liquid Semiconductors* (New York: Plenum)
[19] Meng L J and Dos Santos M P 1993 *Thin Solid Films* **226** 22
[20] Demiryont H, Sites J R and Geib K 1985 *Appl. Opt.* **24** 490
[21] Lai B C, Kung N and Lee J Y J 1999 *Appl. Phys.* **85** 4087
[22] Albrecht W W 1989 *Tantalum and Niobiom* (Berlin: Springer)
[23] Jones S C, Braunlich P, Casper R T, Shen X A and Kelly P 1989 *Opt. Eng.* **28** 1039
[24] Zhao Y A, Gao W D, Shao J D and Fan Z X 2004 *Appl. Surf. Sci.* **227** 275
[25] Yao J K, Shao J D, He H B and Fan Z X 2007 *Appl. Surf. Sci.* **253** 8911
[26] Walker T W, Guenther A H and Nielsen P E 1981 *IEEE J. Quantum Electron.* **17** 2041
[27] Walker T W, Guenther A H and Nielsen P E 1981 *IEEE J. Quantum Electron.* **17** 2053